Logical model specification aided by model- checking techniques: application to the mammalian cell cycle regulation

Pauline Traynard, Adrien Fauré, François Fages, Denis Thieffry

Bioinformatics, YYYY, 0–0
doi: 10.1093/bioinformatics/xxxxx
Advance Access Publication Date: DD Month YYYY
Manuscript Category

Subject Section

Logical model specification aided by model-checking techniques: application to the mammalian cell cycle regulation

Pauline Traynard[1,2], Adrien Fauré[3], François Fages[2] and Denis Thieffry[1,2,*]

[1]Computational Systems Biology team, Institut de Biologie de l'Ecole Normale Supérieure (IBENS), CNRS, Inserm, Ecole Normale Supérieure, PSL Research University, Paris, France.

[2]EPI Lifeware, Inria Inria Saclay Ile-de-France, Palaiseau, France.

[3]Graduate School of Science and Engineering, Yamaguchi University, Yamaguchi, Japan.

*To whom correspondence should be addressed.

Associate Editor: XXXXXXX

Received on XXXXX; revised on XXXXX; accepted on XXXXX

Abstract

Motivation: Understanding the temporal behaviour of biological regulatory networks requires the integration of molecular information into a formal model. However, the analysis of model dynamics faces a combinatorial explosion as the number of regulatory components and interactions increases.

Results: We use model-checking techniques to verify sophisticated dynamical properties resulting from the model regulatory structure in the absence of kinetic assumption. We demonstrate the power of this approach by analysing a logical model of the molecular network controlling mammalian cell cycle. This approach enables a systematic analysis of model properties, the delineation of model limitations, and the assessment of various refinements and extensions based on recent experimental observations. The resulting logical model accounts for the main irreversible transitions between cell cycle phases, the sequential activation of cyclins, and the inhibitory role of Skp2, and further emphasizes the multifunctional role for the cell cycle inhibitor Rb.

Availability: The original and revised mammalian cell cycle models are available in the model repository associated with the public modelling software GINsim (http://ginsim.org/node/189).

Contact: thieffry@ens.fr

Supplementary information: Supplementary data are available on the Bioinformatics website and on the dedicated model webpage.

1 Introduction

Proper understanding of the temporal behaviour of biological regulatory networks requires the integration of heterogeneous molecular and functional data into formal models. Standard quantitative approaches (e.g., differential or stochastic equations) have been recurrently applied to address this issue, but they suffer from the chronic lack of reliable kinetic information. In contrast, qualitative approaches based on Boolean algebra or generalization thereof (Glass & Kauffman, 1973; Thomas, 1973) offer a flexible framework to delineate the main dynamical properties of complex biological regulatory networks. In this framework, dynamical behaviours are represented by transitions between discrete states of the system (see Chaouiya et al., 2012, for more details).

Fauré et al. (2006) defined the first Boolean model for the core network controlling mammalian cell proliferation and demonstrated that the logical framework enables the reproduction of important properties of the highly complex and coordinated system regulating the maintenance and preservation of distinct phases in the cell cycle.

This model accounts for the existence of a cyclic behaviour characterized by the periodic activities of the cyclins, which drive the cell cycle through key transitions by enabling the phosphorylation of a number of substrates by their catalytic partners, the cyclin-dependent kinases (CDKs). Using a hybrid updating scheme relying on the definition of a

limited number of priority classes, Fauré et al (2006) showed that the model dynamics includes two attractors, a stable state and a complex cycle, which can be associated with the quiescent state and cell cycling, respectively. These authors further simulated a series of genetic perturbations and compared them with published data, which revealed several limitations of their model. Since its publication ten years ago, this model has been widely used as a case study for various analytical methods and tools, but to the best of our knowledge its limitations have not been directly addressed, although new models for mammalian cell cycle have recently been published (Fumiã and Martins, 2013; Deritei et al. 2016).

Here, we use a fully asynchronous updating strategy, which allows the consideration of alternative dynamics in the absence of kinetic data, and we rely on formal tools to analyse the resulting complex dynamics in more details. More precisely, we take advantage of powerful model-checking techniques (Clarke et al., 1999) to verify the existence of specific sequences of states (or set of states) in the asynchronous trajectories, formalising dynamical properties such as irreversible transitions between phases of the cell cycle.

We combine an analysis of the asymptotic behaviour of the model, including the impact of reported perturbations (as in Fauré et al, 2006), with the application of model-checking techniques to verify the consistency of the corresponding dynamics with biological observations. We thereby achieve a deeper understanding of the dynamical properties of the original model, as well as of model variants, and highlight their limitations.

Then, based on an extensive review of the literature, we propose several model improvements: refinement of the logical rules, consideration of multilevel variables, and introduction of a novel cell cycle regulator. We use model-checking techniques to assess the impact of each modification on the dynamical properties of the model.

The main features of the logical framework are summarised in Section 2.1. The use of model-checking techniques is then described in Section 2.2. The mammalian core cell cycle network is presented in Section 2.3. The results of our analysis of the original model are presented in Section 3.1, while the rest of Section 3 is devoted to the assessment of the various model improvements considered.

2 Methods

2.1 The logical modelling framework

A logical model is defined by a regulatory graph, where each node represents a regulatory component, and is associated with discrete levels of activity (0, 1, and further integers when justified). Each arc represents a regulatory interaction between the source and target nodes, and is labelled with a threshold and a sign (positive or negative). The model is completed by logical rules (or functions), which assign a target value to each node for each regulator level combination. The resulting dynamics can be represented in terms of a state transition graph (STG), where the nodes denote the states of the system (i.e. vectors giving the levels of activity of all the variables), and the arcs represent state transitions (i.e. changes in variable values, according to the corresponding logical functions) (for more details, see Chaouiya et al., 2012 and Abou-Jaoudé, 2016).

When concurrent variable changes are enabled at a given state, the resulting state transition depends on the chosen updating assumption. With a fully synchronous strategy, all variables are updated through a unique transition. This assumption leads to relatively simple transition graphs and deterministic dynamics. However, this approximation often leads to spurious cyclic attractors.

On the other hand, the fully asynchronous updating assumption considers separately all possible transitions and therefore allows the consideration of alternative dynamics in the absence of kinetic data. The resulting dynamics is more difficult to evaluate.

As in Fauré et al (2006), we use the logical modelling software GINsim to analyse a model of the regulation of the mammalian cell cycle, in particular to identify the attractors and simulate different kinds of genetic perturbations (e.g. gain- or loss-of-function mutants) (Chaouiya et al., 2012; http://ginsim.org).

Furthermore, we rely here on model-checking techniques and the software NuSMV (http://nusmv.fbk.eu/) to analyse complex transition graphs and deepen our understanding of the biochemical circuits underlying such asynchronous dynamics. Noteworthy, the last public release of GINsim includes a function to export logical models into the NuSMV format.

2.2 Dynamical analysis

We refer to three kinds of properties to characterize the dynamics of a logical model and its consistency with biological observations.
To reproduce the oscillatory expressions of proteins along the cell cycle, we require the existence of a cyclic attractor (terminal strongly connected component) in the STG with some constraints on the order of transitions.

Next, existing data on the effects of various experimental perturbations (e.g. mutations) can be used to validate a dynamical model. Indeed, comparing the asymptotic behaviour of a model with or without a perturbation provides interesting insights into the structural properties of the system. The list of the main perturbations used to assess mammalian cell cycle models is provided in Table S1.

Finally, with the help of model-checking techniques, one can easily verify the existence of specific sequences of states or set of states among the possible trajectories simulated with a given updating strategy (from deterministic trajectories with the synchronous updating to branching trajectories with the asynchronous updating).

More precisely, model-checking techniques allows the formal verification of specific dynamical properties and thereby the validation or refutation of a model (Clarke et al., 1999). The formalization of dynamical properties can be done using a temporal logic language such as Computation Tree Logic (CTL). Several powerful model-checking tools are available to evaluate CTL specifications on discrete models.

In this study, we use NuSMV, a symbolic model checker based on Binary Decision Diagrams that provides a description language to specify generic finite state machines (Cimatti et al., 2002). NuSMV has been widely used to check properties on discrete regulatory networks. Chabrier & Fages (2003) introduced symbolic model checking for systems biology using CTL formulae to verify reachability, checkpoints, and oscillation properties for a rule-based model derived from to the molecular map of the mammalian cell cycle proposed by Kohn (1999). Later, Batt et al. (2005) tested conditions leading to a given state, imposing restrictions on sequences of events along the path. In (Batt et al., 2010), model checking with NuSMV was used to solve a parameter search problem for piecewise-affine differential equation models of regulatory networks in order to reproduce observed expression profiles.

Approaches using extensions of standard CTL have been explored, such as Action Restricted CTL (ARCTL), to discriminate between variants of a logical model of T-helper cell differentiation, or to investigate reachability properties between stable states subsequent to changes

of input conditions (Abou-Jaoudé et al., 2015). Another approach implemented in the software ANTELOPE (Arellano et al., 2011) supports Hybrid CTL, an extension of standard CTL with a special binder temporal operator, capable of selecting partly characterised states.

So far, most uses of model checking for logical modelling focused on reachability properties, verifying the existence of a path between a set of initial states and a set of reachable states, with possible restrictions on the paths. Here, we use the model checker NuSMV to verify the existence or the absence of specific state transition paths corresponding to more sophisticated dynamical properties. More specifically, we use the following generic formula to verify the existence of a sequence [S1, S2, …, Sn-1, Sn], following any path starting from a state in S1:

$$!E[\ (S1)\ U\ (S2\ \&\ E[\ (S2)\ U\ (S3\ \&\ \ldots\ E[(Sn\text{-}1)\ U\ (Sn)]\ldots)])];$$

where S1, S2 and S3 denote sets of states defined by constraints on some of the components of the model, while ! stands for the logical negation, E for the existence of a path, and U for the until operator.

The negation is used here for two reasons. First, since a CTL temporal logic property φ holds if all initial states satisfy φ, testing whether its negation ¬φ holds verifies the absence of the specified sequence. Second, a contradiction of ¬φ returns an example of transition path matching the prescribed sequence.

In our study, some of the sequences considered are expected to exist in the asynchronous transition graph, whereas other sequences represent reactions occurring in an incorrect order, and the corresponding dynamical property is then satisfied if the sequence does not exist in the asynchronous STG (cf. Results). The list of sequence properties formalising observed dynamical properties on the cell cycle, and investigated with model checking, is defined in Table S2. The evaluation of each sequence with the symbolic model checker NuSMV takes less than one second on a quad-core laptop.

In the logical framework, the asynchronous assumption relies on a branching definition of time, potentially resulting in different dynamics compatible with the same model. Experimentally-observed sequences of states are expected to exist in the asynchronous trajectories. Otherwise, the model can be safely rejected. In contrast, safety properties (verifying that incorrect sequences do not exist) do not invalidate the model if they are unsatisfied. Incorrect sequences of states that can be exhibited in the asynchronous trajectories do not necessarily indicate a default of the model structure, but might rather point to specific kinetic constraints, which could oppose such spurious trajectories.

Nonetheless, satisfied safety properties represent interesting features of the model. Indeed, a property satisfied in the asynchronous transition graph could always be exhibited in some conditions. The cell cycle represents a particularly interesting case, because the maintenance and preservation of distinct phases is a highly complex and coordinated process. It is regulated by protein synthesis, phosphorylation (through the activity of cyclin-dependent kinases or CDKs) and protein degradation processes (involving ubiquitin ligases). We expect that characteristic dynamical properties, such as checkpoints and irreversible transitions, are robustly encoded in the structure of the corresponding regulatory network. Analysis of a logical model should reveal such properties, despite the absence of detailed kinetic information.

We also show how this approach can aid in refining an existing model. Indeed, at each refinement step, model-checking techniques can be used either to verify correct regulation encoding, or, in the case of uncertain encoding, to discriminate between alternative hypotheses.

2.3 Logical model of the core network controlling mammalian cell cycle

The cell cycle involves a succession of phases governing genome replication (S phase) and cell division (mitosis or M phase), separated by regulated irreversible transitions (checkpoints). Widely conserved among eucaryotes, the underlying core network has been modelled using differential equations for several species (Yeast, Xenopus, mammals), leading to novel insights into its organization and dynamical properties (see e.g. Novák & Tyson, 2004; Gérard & Goldbeter, 2009; Ferrel et al., 2011; Tyson & Novák, 2015; and references therein). However, extension and analysis of such differential models become really difficult as the number of experimentally identified components and interactions increases. This lead to the consideration of simpler, qualitative but nevertheless rigorous formal approaches, using discrete formalisms (see e.g. Li et al., 2004; Bornholdt, 2008; Irons, 2009; Fauré et al., 2009; Mombach et al., 2014).

The present study is based on the first Boolean model of the mammalian cell cycle (Fauré et al. 2006), which demonstrated that the logical framework enables the reproduction of important dynamical properties. Fauré et al. (2006) defined a Boolean model for the core network driving the entry of mammalian cells into cell cycle, based on the differential model proposed by Novák and Tyson in 2004. For proper logical rules, this model accounts for the existence of a quiescent stable state, as well as for a cyclic attractor characterized by the periodic activities of the cyclins, which drive the cell cycle through key transitions by enabling the phosphorylation of a number of substrates by their catalytic partners, the cyclin-dependent kinases (CDKs). Cyclin D (called CycD and corresponding to an input in the model) is the main target of the growth factors that push a cell out of its quiescent state to enter the cell cycle. Cyclin E (CycE) regulates the transition between the G1 and S phases. Cyclin A (CycA) controls S phase and its progression into G2 phase. Finally, cyclin B (CycB) is in charge of the transition from G2 phase to mitosis and triggers the division of the cell.

The model of Fauré et al. (2006) further includes the three main inhibitors of the cell cycle: the retinoblastoma protein Rb, the CDK inhibitor p27/Kip1 (called p27 hereafter), and the proteasome complex represented by its two co-activators Cdh1 and Cdc20. However, this seminal model considered CycD sufficient to completely inhibit p27 and Rb. Hence, these inhibitors were kept inactive along the whole cyclic attractor, whereas, according to experimental data, these factors should be active in G1 phase, and inactive in the rest of the cell cycle (Rivard et al., 1996; Nelson et al. 1997).

This model also accounts for the role of the E2 ubiquitin conjugating enzyme UbcH10, which participates in Cdh1 dependent degradation of CycA. This extension of the original differential model explains how the auto-ubiquitination of UbcH10 likely prevents CycA from degradation by the APC in G1 phase.

Finally, Fauré et al. (2006) considered a list of documented perturbations to validate their model. However, the simulations of several perturbations did not match experimental observations. In particular, the effect of a loss-of-function of CycE was not adequately reproduced.

3 Results

In this study, we first investigate the asynchronous dynamics of the model of Fauré et al (2006) using model-checking techniques and perturbation analysis. We further rely on an extensive review of the literature to identify relevant novel information. Next, we systematically

assess tentative model refinements and extensions to improve matching with reported data.

We model the potential roles of different phosphorylation states of Rb (Lundberg & Weinberg, 1998) through the use of a ternary node (i.e. taking the value 0, 1 and 2). We also assign a ternary node to p27 in order to account for its significant but incomplete degradation in the presence of CycD (in the absence of CycA and CycE). We further assess the inclusion of Skp2, an ubiquitin ligase complex subunit involved in the degradation of several proteins in the model, which links three key inhibitors of the cell cycle and constitutes an additional pathway by which Rb can arrest the progression of the cell cycle (Binné et al., 2007; Liu et al., 2008). The resulting regulatory graph is depicted in Figure 1, while the corresponding logical rules are listed in Table 1.

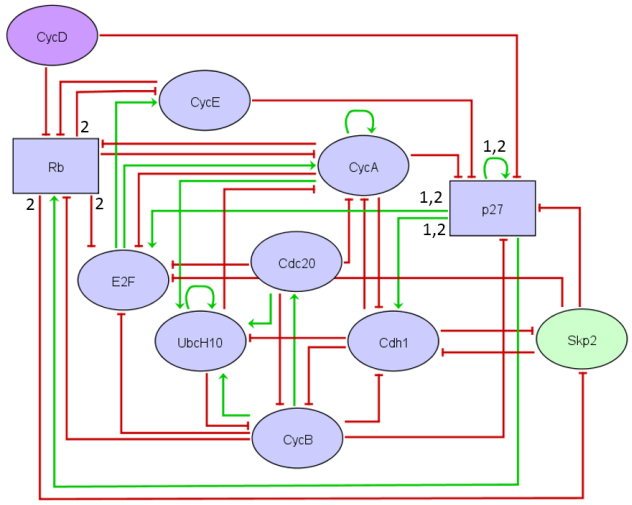

Fig. 1. Regulatory graph for the revised mammalian cell cycle model. All nodes are Boolean (ovals), excepting Rb and p27 (rectangles), which are associated with ternary variables. CycD (purple) corresponds to an input (unregulated) node, while Skp2 (green) is newly considered in this study. Green and red arcs denote positive and negative interactions, respectively. Interactions involving thresholds higher than 1 are labelled accordingly. See Table 1 and text for the description of the modifications of the original model.

3.1 Verification and limitations of the original model

In their seminal study, Fauré et al. (2006) showed that the proposed model leads to two attractors: a stable state corresponding to the quiescent state (with CycD OFF), and a complex attractor corresponding to cell cycling (with CycD ON, with p27 and Rb OFF during the whole cycle). They further simulated various genetic perturbations, with encouraging results, although not fully consistent with published data.

To check in more details the consistency of the model with our current knowledge on the sequential activation of the model components, we perform a refined analysis of the asynchronous dynamics.

Table 1. Logical rules associated with each node of the mammalian cell cycle model (Figure 1).

Node	Target	Logical function
Cdc20	1	CycB
Cdh1	1	(!CycA | (p27:1 & !Skp2) | p27:2) & (!CycB | p27)
CycA	1	(E2F & !Rb | CycA) & (!UbcH10 | (!Cdh1 & !Cdc20))
CycB	1	(!UbcH10 | !Cdc20) & !Cdh1
CycE	1	E2F & !Rb
E2F	1	!Rb & (!CycA | (p27:1 & !Skp2) | p27:2) & !(Cdc20 & CycB)
p27	1	CycD & ((!CycB & (!CycA | p27) & (!CycE | (p27:2 & !CycA))) | !Skp2)
	2	!CycD & ((!CycB & (!CycA | p27) & (!CycE | (p27:2 & !CycA))) | !Skp2)
Rb	1	(CycD & !CycE & !CycA & !CycB) | (!CycD & p27 & CycE & CycA & CycB) | (CycD & (CycE | CycA | CycB) & p27)
	2	(!CycD & !CycE & ((!CycA & !CycB) | p27)) |(!CycD & p27 & CycE & (!CycA | !CycB))
Skp2	1	!Cdh1 | !Rb
UbcH10	1	!Cdh1 | (Cdh1 & UbcH10 & (CycA | Cdc20 | CycB))

The logical operators NOT, AND and OR are denoted by !, & and |, respectively. Changes in the model rules compared to those of the original model by Fauré et al (2006) are coloured in blue (in particular, Skp2 was not included in the original model).

First, we define a set of constraints on the order of activation and inactivation of the cyclins along the cell cycle. These constraints correspond to a sequence starting with a state associated with G1 (all cyclins OFF but CycD, and Cdh1 ON), followed by the sequential activation of CycE, CycA, and CycB, interspaced by the sequential inactivation of these three cyclins in the same order (see Table S2, sequence 1).

This sequence of states can be refined to further account for the sequential activation of the other model components, excepting p27 and Rb, which remain inactive in the cyclic attractor of the model of Fauré et al. (2006) (Figure 2). The resulting sequence encompasses 14 states, where the S, G2 and M phases correspond to the activation of CycE, CycA and CycB, respectively. Using model checking, we can verify that this sequence exists in the asynchronous state transition graph (for CycD = 1), showing that the asynchronous dynamics of the original model is compatible with experimental observations.

However, the asynchronous graph further includes altered sequences contradicting observed phenotypes (see the asterisks denoting updating calls according to the original model in Figure 2). In particular, CycA could be activated first at the beginning of the cell cycle instead of CycE (Figure 2, state 2; Table S2, sequence 6). Similarly, there is no constraint on the order of the inactivations of CycA and CycB at the end of the cell cycle (Figure 2, state 10; Table S2, sequence 9). Furthermore, the activation of CycB, experimentally observed in late G2, can occur before the degradation of CycE, supposedly occurring in S phase (Figure 2, states 5 and 6; sequence 8). And although this event is presumably irreversible, in the model, CycB can be reactivated soon after it is degraded at the end of mitosis, before the beginning of a new cycle (Figure 2, state 13; Table S2, sequences 5 and 7). These findings point toward structural or kinetic limitations of the model.

Interestingly, the absence of commutation orders at some states reveals the existence of specific constraints in the asynchronous trajectories. For example, CycE is irreversibly inactivated at the G1/S transition (Figure 2, state 7; Table S2, sequence 3), while CycA is irreversibly inactivated at M phase (Figure 2, state 11; Table S2, sequence 4). This shows that the corresponding properties are encoded in the model structure without relying on kinetic properties.

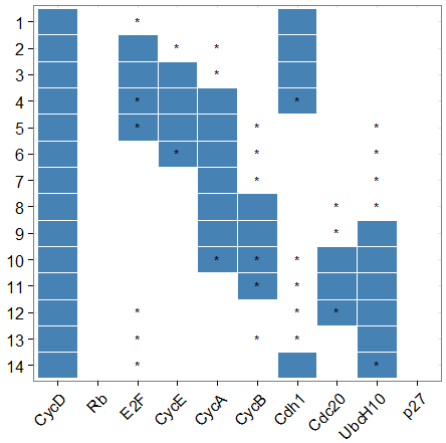

Fig. 2. Single asynchronous sequence of states corresponding to the mammalian cell cycle according to the model of Fauré et al. (2006). This sequence encompasses 14 successive states along the cell cycle, with active nodes (level 1) in blue and inactive nodes (level 0) in white. The asterisks denote updating calls for the corresponding components (columns) and states (rows), corresponding to possible alternative paths, based on the published logical rules. States 1, 3, 7, and 11 correspond to G1, S, G2 and M phases.

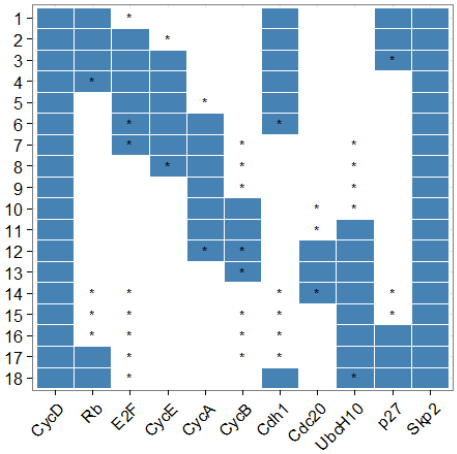

Fig. 3. Single asynchronous state transition sequence corresponding to a complete wild type mammalian cell cycle for the revised model shown in Figure 1, along with the logical rules provided in Table 1. This sequence encompasses 18 successive states along the cell cycle, with active nodes (level 1) in blue, and inactive nodes (level 0) in white. The asterisks denote updating calls for the corresponding components (columns) and states (rows) according to the rules listed in Table 1, corresponding to possible alternative paths. States 1, 3, 9, and 13 correspond to middle G1, S, G2 and M phases.

3.2 Model refinement

The CDK inhibitor p27 plays a critical role in several phases of the cell cycle, as well as in the maintenance of the quiescent state. It binds CycE and CycA, thereby inhibiting their activities. This inhibitory activity is modelled by opposite regulations on the targets of CycE and CycA. In contrast, the complex formed by p27 and CycD retains the activity of CycD. Since the cyclins are in competition for complexation with p27, the initial model considered a direct inhibition of p27 by CycD to reflect the sequestration of the inhibitor by CycD during the cell cycle. This causes p27 to be completely inactive in presence of CycD, while it is released and active in absence of the input (i.e. in the quiescent state). This approximation overlooks the role of p27 in the transition from G1 to S. In fact, the complete activation of CycE is a progressive process, slowed down by both Rb and p27, which are both negative regulators of CycE. Indeed, Rb binds to the transcription factor E2F, thereby inhibiting its ability to activate the synthesis of CycE, whereas p27 directly binds to CycE:CDK2 complex and thereby blocks its activity. Rb and p27 are both phosphorylated by CycE, leading to the inactivation of Rb and to the proteasome-dependent degradation of p27. These factors are thus involved in a positive circuit enabling the full activation of the kinase and ultimately entry into S phase (Kotoshiba et al., 2005).

In order to account for this mechanism, we associate a ternary node with p27 and distinguish two activation levels, in the presence versus the absence of CycD. We further modify p27 rule to better account for the inhibitory effect of CycE (Montagnoli et al., 1999) (cf. Table 1).

Simulation of the updated model results in an asynchronous attractor with cycling p27 activity (values 0 and 1) in the presence of CycD (see Figure 3). The timing of p27 inactivation can be assessed by verifying the existence of a proper sequential activation path for CycE, CycA and p27, between phases G1 and S for the updated model (Table S2, sequence 11). Indeed, the activity of p27 is correctly constrained at the G1/S transition: it cannot be inactivated before the activation of its inhibitor CycE, while its inactivation is necessary for the activation of CycA (Table S2, sequences 12 and 13; States 2 and 4 in Figure 3).

Careful reconsideration of each regulation rule further led us to question the inhibition of E2F by CycB (see also Deritei et al., 2016). Although E2F has been shown to be inhibited by CycA through direct binding, this is not the case for CycB (Krek et al., 1994). However, Peart et al. (2010) have found that Cdc20, and to a lesser extend Cdh1, is responsible for degrading E2F in early mitosis, when E2F is freed from complexes with DP1. It has been proposed by Weis et al. (2014) that phosphorylation by CycB enables the release of E2F, exposing it to Cdc20.

Combining the use of logical modelling and model-checking techniques greatly facilitates the assessment of such hypotheses. Considering an inhibition of E2F by the conjunction of Cdc20 and CycB activities, we verify the ordering of cyclin activities (and thus correct mitosis exit) in the presence or absence of this novel interaction. In the absence of E2F inhibition by Cdc20, CycE can be synthesised before the degradation of CycB, which is not the case when this inhibition is taken into account (cf. Table S2, sequence 10; states 9 to 18 in Figure 3). Hence, the delay observed between CycB degradation after mitosis and CycE activation during G1-phase could be ensured by this mechanism.

We further reconsider the potential role of Cdc20 in the activation of Cdh1. These two proteins take part in the anaphase-promoting complex (APC) and are activated sequentially during the G2 and M phases to promote the degradation of the mitotic cyclins A and B. Since Cdc20 participates in the degradation of CycA, which inhibits Cdh1 by phosphorylation, there is an indirect activation of Cdc20 by Cdh1. As Cdh1 has a broader spectrum than Cdc20, it completes CycA and CycB inactivation, and further inactivates Cdc20 (Meyer & Rape, 2011). Using NuSMV, we could verify that the direct activation of Cdh1 by Cdc20 can be eliminated without impacting on relevant model properties (the resulting rule for Cdh1 is given in Table 1).

3.3 Multiple forms and roles of Rb

The protein Rb is a major cell cycle inhibitor and tumour suppressor. It is regulated by numerous stimuli, which are channeled through CDK regulation of Rb phosphorylation. The un-phosphorylated protein binds

to the transcription factor E2F, thereby acting as a growth suppressor and preventing progression through the cell cycle. When phosphorylated, Rb releases E2F, which activates the synthesis of CycE and CycA. Recent findings show that the phosphorylation of Rb is a progressive process (Henley et al., 2012). The phosphorylation of Rb begins in early G1 phase, involving CycD:CDK complexes (Narasimha et al., 2014). This allows some E2F to be released and initiates the transcription and subsequent production of CycE. The CycE:CDK2 kinase activity then leads to hyper-phosphorylation of Rb. As the majority of phosphorylation sites on Rb need to be modified to abrogate E2F binding, different activities are associated with different phosphorylation levels of Rb, with CycE playing a key role in driving the cell cycle into S-phase. Later on, Rb is maintained in a hyper-phosphorylated state by CycA and CycB complexes in S, G2, and M phases.

Refining the description of Rb with a multivalued node was already suggested by Fauré et al. (2006). Hence, we introduce a ternary node for Rb, with the levels 0, 1 and 2 corresponding to the hyper-phosphorylated, partly-phosphorylated and un-phosphorylated states respectively (the corresponding logical rules are defined in Table 1). The cyclins phosphorylate and inhibit Rb. In the absence of cyclins, Rb is un-phosphorylated (level 2). CycD alone initiates the partial phosphorylation at the beginning of the cell cycle, and thus pushes Rb down to the level 1. It requires the assistance of another cyclin to complete this phosphorylation, forcing Rb down to the level 0, in the absence of p27. CycA and CycB have symmetrical roles, keeping Rb hyper-phosphorylated during S, G2 and M phases. p27 binds to the CycA/E/B:CDK complexes and inhibits their kinase activities, thereby indirectly activating Rb. Although p27 can also bind CycD:CDK complexes, it does not impair the corresponding kinase activity. A saturation of p27 inhibitory activity by the different cyclins is further considered in the corresponding logical rule (see Table 1).

Interestingly, this model extension provides a mechanism explaining the requirement of CycE for cell cycle viability, as well as the sequential synthesis of CycE and CycA. The synthesis of both cyclins is activated by E2F, but their expressions peak in G1 phase and S phase, respectively (Lees et al., 1992; Wong et al., 2014). We model this sequential activation by considering differential effects of Rb depending on its phosphorylation state. The complexation of Rb and E2F is modelled with a direct inhibition of E2F by Rb, along with negative regulations of E2F targets CycE and CycA (as in Fauré et al., 2006). Setting different thresholds of activity for these interactions, namely threshold 2 for E2F and CycE, and threshold 1 for CycA, ensures that the synthesis of CycA can be activated only when Rb is hyper-phosphorylated and E2F is completely released.

The delayed synthesis of CycA relatively to the synthesis of CycE can be verified with NuSMV (Table S2, sequence 6; states 2 to 4 in Figure 3). Indeed, the incorrect sequence with CycA activated before CycE no longer exists in the asynchronous STG of the revised model. Hence, our model provides an explanation for the observed sequential activation of CycE and CycA in the cell cycle, which relies on a robust mechanism involving the feedforward motif that drives the complete phosphorylation of Rb and the progression into S phase.

The requirement of CycE for cell cycle viability might depend on cellular context. CycE is known to participate in the phosphorylation of Rb (Weinberg, 1995). However, observations on CycE-deficient cells highlight a crucial role of CycE in specific situations. Geng et al. (2003) reported that CycE-deficient cells can maintain active proliferation but are unable to reenter the cell cycle from the quiescent G0 state. Ohtsubo et al. (1995) further report that inhibition of CycE in G1 blocks the entry in S phase in human cells and further arrests the cell cycle.

For CycE knock-out, the simulation of the original model did not result in cell cycle arrest, because the activity of CycA, which drives the cell cycle into G2 phase, was independent from CycE. In contrast, our modified model predicts an arrest of the cell cycle in phase G1, where CycA is inhibited by Rb (Table S1). This simulation emphasises the role of the circuit involving Rb, CycE and p27 in driving the cell cycle through the S phase and beyond.

A similar perturbation was introduced in a recent study, where cancer cells are treated with a specific CycE/A inhibitor, resulting in a cell cycle arrest with an increased accumulation of p27 and hypo-phosphorylation of Rb (Dai et al., 2013). With the revised model, the simulation of a double perturbation of CycE and CycA leads to consistent results, while the same perturbation in the initial model leads to a cell cycle arrest with phosphorylated Rb (Rb=0) and no p27 accumulation (p27=0) (Table S1).

3.4 Role of UbcH10 in mitosis

The anaphase-promoting complex (APC) coordinates mitosis and G1 by sequentially promoting the degradation of key cell-cycle regulators. APC is represented in the model by Cdh1 and Cdc20. The degradation of several targets of either Cdh1 or Cdc20 is assisted by the ubiquitin-conjugating enzyme 2C (UbcH10, also called UBE2C), a component of the ubiquitin proteasome system.

While the initial model accounted for the fact that UbcH10 is necessary for Cdh1-dependent degradation of CycA (Rape & Kirshner, 2004), UbcH10 might also be required for the destruction of mitotic cyclins and other mitosis-related substrates, including CycB (Rape et al., 2006). We encode this putative mechanism by updating the logical rule associated with the node CycB (cf. Table 1). Adding the intervention of UbcH10 for the degradation of CycB enables a consistent simulation of UbcH10 KO (Townsley et al., 1997). Indeed, using NuSMV, one can verify that there is no asynchronous sequence going through G2 and M phase (driven by CycA and CycB) in absence of UbcH10 (starting from an initial state corresponding to S phase) (Table S2, sequence 18), which is not the case for the model of Fauré et al. (2006).

UbcH10 is probably also involved in Cdh1-dependent degradation of CycB. In the absence of definitive experimental data, we can test the impact of this mechanism on cell cycle dynamics by applying model-checking techniques on model variants with alternative rules for CycB. In Table 1, we have retained the rule satisfying the largest number of constraints.

3.5 Role of Skp2

Within the logical framework, it is relatively easy to extend a model in order to consider novel regulatory components and interactions. Recent evidence points to the existence of an E2F-independent proliferative control mechanism, which involves the F-box protein Skp2, a substrate recognition subunit of the SCF ubiquitin ligase complex that targets p27 for degradation (Dick & Rubin, 2013). Briefly, Skp2 promotes the degradation of phosphorylated p27 by CycE and CycA associated CDKs. Rb binds to Cdh1 and thereby participates in the ubiquitin-mediated degradation of Skp2 (Binné et al., 2007; Liu et al., 2008). This mechanism links the three key cell cycle repressors Rb, p27 and Cdh1, and provides an additional mechanism by which Rb can arrest the cell cycle. Consequently, we define a novel node representing Skp2 in the model, negatively regulated by Cdh1 and (non-phosphorylated) Rb, and inhibiting p27. The presumptive correct sequence of states for the revised model is shown in Figure 3.

The performances of this revised model have been assessed by checking the consistency between model perturbations and experimental data. In particular, Ji et al. (2004) described the partial penetrance of Rb mutation RbR661W, which impedes E2F repression, and effectively shuts down the Rb-E2F pathway. These authors further found that RbR661W retains the ability to arrest the cell cycle at the G1/S transition, with p27 accumulation. They verified that the ability of Rb to interact with Skp2-p27 was preserved in this mutant. In the logical framework, it is possible to model this subtle perturbation by specifically suppressing the regulation of E2F, CycE and CycA by Rb.

In another experiment, p27 antisense treatment was shown to prevent G1 arrest by Rb, indicating that p27 is required for Rb-mediated G1 arrest. This can be modelled by considering another model perturbation (knock-down of p27), with simulation results consistent with experimental data (see Table 2).

Table 2. Assessment of properties of the original and revised mammalian cell cycle model.

Genetic perturbation	Observed Phenotype	Initial model	Revised model
RbR661W	Viable cell cycle in the presence of growth factors, cell cycle arrest and p27 accumulation in their absence.	Inconsistent	OK
Rb induction	Cell cycle arrest with present CycE and CycA	Inconsistent	OK
p27 KO	Cell cycle in absence of growth factors.	Inconsistent	OK
Skp2 KO	Cell cycle arrest or endoreplication with accumulation of cyclin E and p27.	Skp2 absent	OK
Skp2 KO p27 KO	Cell cycle in the presence of growth factors, cell cycle arrest accumulation of CycE in their absence.	Skp2 absent	OK but no accumulation of CycE

Moreover, Skp2 specific perturbations have been reported, which can also be qualitatively reproduced with our model. In particular Skp2 KO has been shown to lead to severe proliferation defects, with accumulation of both CycE and p27 (Kotoshiba et al., 2014; Nakayama et al., 2000). Consistently, the simulation of this perturbation leads to a steady state with CycE and p27 both active (level 1). The rescue of Skp2 loss-of-function by the deletion of p27 (Nakayama et al., 2004) is reproduced by the model, but does not account for CycE accumulation (see Table 2).

Skp2 is known to degrade free CycE, but CycE complexed with CDK2 is protected from Skp2-dependent degradation (Nakayama et al., 2000). In our model, the component CycE represents the complex CycE:CDK2, and the negative regulation of CycE by Skp2 is thus not taken into account. In this respect, our perturbation simulation results suggest an alternative mechanism by which CycE could be accumulated in Skp2 mutants, presumably involving p27 binding to CycE. The resulting complexes could inhibit CycE activity and arrest the cell cycle before the transition toward S phase.

Finally, the updated model can be used to interrogate the regulation of Skp2 by E2F. The observation that E2F directly activates transcription of skp2 gene (Assoian & Yung, 2008) led us to analyse a model variant including a positive regulation by E2F opposing the inhibition by Rb. However, our model checking analysis of the dynamics of this variant suggests that further refinements would be needed to account for this interaction without loosening other necessary constraints. Indeed, although this model variant allows Skp2 to oscillate in the cyclic attractor, we further observe a destabilisation of CycE and CycA. Hence, further experimental details on Skp2 regulation and stability would be needed before integrating this interaction in our mammalian cell cycle model.

4 Conclusions and prospects

4.1 Model refinement

Refining a model is an iterative process, during which it is important to check at each step that all relevant properties satisfied by the original model are preserved, while novel properties are further accounted for. In this study, we have refined a logical model of the mammalian cell cycle to account for recent data pointing to novel regulatory components and interactions. Each model update was evaluated using formal model-checking techniques to assess the conservation of documented dynamical properties, in particular regarding the temporal ordering of cyclin activities, for the wild type cycle, as well as for various genetic perturbations. In this respect, we provide the complete lists of perturbations (Table S1) and dynamical properties (Table S2) evaluated on all model variants as supplementary material. Interestingly, the revised model matches several novel biologically relevant properties in comparison with the original one.

However, a careful analysis of our refined model already points to some limitations. In particular, the timing of the degradation of CycB relative to the other cyclins is not fully determined (cf. State 12 in Figure 3). This raises the question of what refinement could ensure the correct timing for CycB inactivation. Further experimental perturbation studies could point to possible mechanisms. For example, the use of stabilized cyclins in proliferating cells could help to conclude whether the degradation of CycE, CycA and CycB are necessary for the progression into the next phase.

Another limitation of the model is the existence of two stable states corresponding to cell quiescence, differing in the level of CycA (level 0 or 1), and due to the stability of CycA in the model in absence of all its regulators. The modelling of the regulation of CycA degradation (in free form versus CycA:CDK complex) clearly needs to be further refined.
Finally, as mentioned above, we have still to refine the logical modelling of the regulation of Skp2 by E2F, which should preserve the correct temporal ordering of CycE and CycA activities.

4.2 Prospects

Our refined model takes into account the most notable components of the mammalian cell cycle network. However, this model should be further updated in the light of novel experimental data. Besides Skp2, several additional proteins have been involved in the regulation of the G2 phase, such as Aurora, Plk1, Emi1, which have not yet been considered in our model because their roles and regulation are still uncertain. These factors will be possibly incorporated in the model once more precise mechanistic information becomes available.

At some point, one could consider more subtle kinetic aspects to enforce the fine temporal regulation of the cyclins, which would require more quantitative approaches. One straightforward possibility would be to use the software MaBoSS to perform stochastic simulations, relying on rough estimation of relative component transition rates (Stoll et al., 2012). In this respect, the development version of GINsim includes a functionality enabling the export of logical models into MaBoSS format.

Our model could also be refined to fit data concerning specific cell types, or to study the effect of multiple perturbations associated with cancer (e.g. Grieco et al., 2013; Mombach et al., 2014; Floback et al., 2015; Remy et al., 2015). It can be used as a starting point for subsequent studies, using the model-checking approach delineated here in order to increment and assess successive model versions. In this respect,

we provided our current model in two computer readable formats (GINsim format, including extensive annotations, along with an SBML export (http://ginsim.org/node/189).

Funding

This work has received support under the program *Investissements d'Avenir* launched by the French Government and implemented by ANR with the references ANR- 10- LABX- 54 MEMOLIFE and ANR- 11- IDEX- 0001- 02 PSL* Research University. PT has been funded by an AMX doctoral grant from the *Ministère de l'Education Nationale, de l'Enseignement Supérieure et de la Recherche*, France. AF has received support from Kakenhi Grant-in-aid for Young Scientists (B): 24710230.

Conflict of Interest: none declared.

References

Abou-Jaoudé, W., Traynard, P., Monteiro, P. T., Saez Rodriguez, J., Helikar, T., Thieffry, D., Chaouiya, C. (2016). Logical modeling and dynamical analysis of cellular networks. *Front. Genet.*, **94**(7).

Abou-Jaoudé, W., Monteiro, P. T., Naldi, A., Grandclaudon, M., Soumelis, V., Chaouiya, C., and Thieffry, D. (2015). Model checking to assess T-helper cell plasticity. *Front. Bioeng. Biotechnol.*, **2**(Suppl. 1), 86.

Arellano, G., Argil, J., P., Rosenblueth, D. A., Azpeitia, and Alvarez-Buylla, E., Benítez, M., Carrillo, M., Góngora, E. R. (2011). "Antelope": a hybrid-logic model checker for branching-time Boolean GRN analysis. *BMC Bioinformatics*, **12**(1), 490.

Assoian, R. K. and Yung, Y. (2008). A reciprocal relationship between Rb and Skp2: implications for restriction point control, signal transduction to the cell cycle and cancer. *Cell Cycle*, **7**(1), 24–27.

Batt, G., Ropers, D., de Jong, H., Geiselmann, J., Mateescu, R., Page, M., and Schneider, D. (2005). Validation of qualitative models of genetic regulatory networks by model checking : Analysis of the nutritional stress response in Escherichia coli. *Bioinformatics*, **21**(Suppl.1), i19–i28.

Batt, G., Page, M., Cantone, I., Goessler, G., Monteiro, P., and de Jong, H. (2010). Efficient parameter search for qualitative models of regulatory networks using symbolic model checking. *Bioinformatics*, **26**(18), i603–i610.

Binné, U. K., Classon, M. K., Dick, F. A., Wei, W., Rape, M., Kaelin, W. G., Naar, A. M., and Dyson, N. J. (2007). Retinoblastoma protein and anaphase-promoting complex physically interact and functionally cooperate during cell-cycle exit. *Nat. Cell Biol.*, **9**(2), 225–232.

Bornholdt, S. (2008). Boolean network models of cellular regulation: prospects and limitations. *J. R. Soc. Interface*, **5**(Suppl 1), S85–S94.

Chabrier, N. and Fages, F. (2003). Symbolic model checking of biochemical networks. In C. Priami, editor, *CMSB'03: Proceedings of the first workshop on Computational Methods in Systems Biology*, Vol. 2602 of Lecture Notes in Computer Science, pp. 149–162, Rovereto, Italy. Springer-Verlag.

Chaouiya, C., Naldi, A., and Thieffry, D. (2012). Logical modelling of gene regulatory networks with ginsim. *Methods Mol. Biol.*, **804**, 463–79.

Cimatti, A., Clarke, E., Enrico Giunchiglia, F. G., Pistore, M., Roveri, M., Sebastiani, R., and Tacchella, A. (2002). Nusmv 2: An opensource tool for symbolic model checking. In *Proceedings of the International Conference on Computer-Aided Verification, CAV'02, Copenhagen, Danmark*.

Clarke, E. M., Grumberg, O., and Peled, D. A. (1999). Model Checking. MIT Press.

Dai, L., Liu, Y., Liu, J., Wen, X., Xu, Z., Wang, Z., Sun, H., Tang, S., Maguire, A. R., Quan, J., Zhang, H., and Ye, T. (2013). A novel CyclinE/CyclinA-CDK Inhibitor targets p27Kip1 degradation, cell cycle progression and cell survival: Implications in cancer therapy. *Cancer Lett.*, **333**(1), 103–112.

Deritei D., Aird W. C., Ercsey-Ravasz M., Regan E. R. (2016). Principles of dynamical modularity in biological regulatory networks. *Sci. Rep.* **16**(6), 21957.

Dick, F. a. and Rubin, S. M. (2013). Molecular mechanisms underlying RB protein function. *Nat. Rev. Mol. Cell Biol.* **14**(5), 297–306.

Fauré, A., Naldi, A., Chaouiya, C., and Thieffry, D. (2006). Dynamical analysis of a generic Boolean model for the control of the mammalian cell cycle. *Bioinformatics*, **22**(14), e124–e131.

Fauré, A., Naldi, A., Lopez, F., Chaouiya, C., Ciliberto, A., and Thieffry, D. (2009). Modular logical modelling of the budding yeast cell cycle. *Mol. Biosyst.*, **5**, 1787–1796.

Ferrell, J. E., Tsai, T. Y.-C., and Yang, Q. (2011). Modeling the cell cycle: why do certain circuits oscillate? *Cell*, **144**(6), 874–885.

Flobak, A., Baudot, A., Remy, E., Thommesen, L., Thieffry, D., Kuiper, M., and Lægreid, A. (2015). Discovery of drug synergies in gastric cancer cells predicted by logical modeling. *PLoS Comput. Biol.*, **11**(8), e1004426.

Fumia, H. F., & Martins, M. L. (2013). Boolean Network Model for Cancer Pathways: Predicting Carcinogenesis and Targeted Therapy Outcomes. *PLoS ONE*, **8**(7):e69008.

Geng, Y., Yu, Q., Sicinska, E., Das, M., Schneider, J. E., Bhattacharya, S., Rideout, W. M., Bronson, R. T., Gardner, H., and Sicinski, P. (2003). Cyclin E ablation in the mouse. *Cell*, **114**(4), 431–443.

Gérard, C. and Goldbeter, A. (2009). Temporal self-organization of the cyclin/cdk network driving the mammalian cell cycle. *PLoS Comput. Biol.*, **106**(51), 21643–21648.

Glass, L. and Kauffman, S. A. (1973). The logical analysis of continuous, non-linear biochemical control networks. *J. Theor. Biol.*, 39**(**1), 103–129.

Grieco, L., Calzone, L., Bernard-Pierrot, I., Radvanyi, F., Kahn-Perles, B., and Thieffry, D. (2013). Integrative modelling of the influence of MAPK network on cancer cell fate decision. *PLoS Comput. Biol.*, **9**(10), e1003286.

Henley, S. A. and Dick, F. A. (2012). The retinoblastoma family of proteins and their regulatory functions in the mammalian cell division cycle. *Cell Div.*, **7**(1), 10.

Irons, D. (2009). Logical analysis of the budding yeast cell cycle. *J. Theor. Biol.*, **257**(4), 543–559.

Ji, P., Jiang, H., Rekhtman, K., Bloom, J., Ichetovkin, M., Pagano, M., and Zhu, L. (2004). An Rb-Skp2-p27 pathway mediates acute cell cycle inhibition by Rb and is retained in a partial-penetrance Rb mutant. *Mol. Cell*, **16**(1), 47–58.

Kohn, K. W. (1999). Molecular interaction map of the mammalian cell cycle control and DNA repair systems. *Mol. Biol. Cell*, **10**(8), 2703–2734.

Kotoshibai, S., Kamura, T., Hara, T., Ishida, N., and Nakayama, K. I. (2005). Molecular dissection of the interaction between p27 and Kip1 ubiquitylation-promoting complex, the ubiquitin ligase that regulates proteolysis of p27 in G1 phase. *J. Biol. Chem.*, **280**(18), 17694–17700.

Kotoshiba, S., Gopinathan, L., Pfeiffenberger, E., Rahim, A., Vardy, L. A., Nakayama, K., Nakayama, K. I., and Kaldis, P. (2014). p27 is regulated independently of Skp2 in the absence of Cdk2. *Biochim. Biophys. Acta*, **1843**(2), 436–445.

Krek, W. (1994). Negative regulation of the growth- promoting transcription factor E2F-1 by a stably bound cyclin A-dependent protein kinase. *Cell*, **78**(1), 161–172.

Lees, E., Faha, B., Dulic, V., Reed, S. I., and Harlow, E. (1992). Cyclin E/cdk2 and cyclin A/cdk2 kinases associate with p107 and E2F in a temporally distinct manner. *Genes Dev, 6(10)*, 1874–1885.

Li, F., Long, T., Lu, Y., Ouyang, Q., and Tang, C. (2004). The yeast cell-cycle network is robustly designed. *Proc. Natl. Acad. Sci. U.S.A.*, **101**(14), 4781–4786.

Liu, Y., Perdreau, S. a., Chatterjee, P., Wang, L., Kuan, S.-F., and Duensing, A. (2008). Imatinib mesylate induces quiescence in gastrointestinal stromal tumor cells through the CDH1-SKP2-p27Kip1 signaling axis. *Cancer Res.*, **68**(21), 9015–9023.

Lundberg, A. S. and Weinberg, R. A. (1998). Functional inactivation of the retinoblastoma protein requires sequential modification by at least two distinct cyclin-cdk complexes. *Mol. Cell. Biol.*, **18**(2), 753–761.

Meyer, H. J. and Rape, M. (2011). Processive ubiquitin chain formation by the anaphase-promoting complex. *Semin. Cell Dev. Biol.*, **22**(6), 544–550.

Mombach, J. C. M., Bugs, C. A., and Chaouiya, C. (2014). Modelling the onset of senescence at the g1/s cell cycle checkpoint. *BMC Genomics*, **15** Suppl 7, S7.

Montagnoli, A., Fiore, F., Eytan, E., Carrano, A. C., Draetta, G. F., Hershko, A., and Pagano, M. (1999). Ubiquitination of p27 is regulated by CDK dependent phosphorylation and trimeric comples formation. *Genes Dev.*, **13**, 1181–1189.

Nakayama, K., Nagahama, H., Minamishima, Y. A., Matsumoto, M., Nakamichi, I., Kitagawa, K., Shirane, M., Tsunematsu, R., Tsukiyama, T., Ishida, N., Kitagawa, M., and Hatakeyama, S. (2000). Targeted disruption of Skp2 results in accumulation of cyclin E and p27(Kip1), polyploidy and centrosome overduplication. *EMBO J.*, **19**(9), 2069–2081.

Nakayama, K., Nagahama, H., Minamishima, Y. a., Miyake, S., Ishida, N., Hatakeyama, S., Kitagawa, M., Iemura, S. I., Natsume, T., and Nakayama, K. I. (2004). Skp2-Mediated degradation of p27 regulates progression into mitosis. *Dev. Cell*, **6**, 661–672.

Narasimha, A. M., Kaulich, M., Shapiro, G. S., Choi, Y. J., Sicinski, P., and Dowdy, S. F. (2014). Cyclin D activates the Rb tumor suppressor by mono-phosphorylation. *eLife*, **3**, e02872.

Nelson, D. A., Krucher, N. A., and Ludlow, J. W. (1997). High molecular weight protein phosphatase type 1 dephosphorylates the retinoblastoma protein. *J. Biol. Chem.*, **272**(7), 4528–4535.

Novák, B. and Tyson, J. J. (2004). A model for restriction point control of the mammalian cell cycle. *J. Theor. Biol.*, **230**, 1383–1388.

Ohtsubo, M., Theodoras, a. M., Schumacher, J., Roberts, J. M., and Pagano, M. (1995). Human cyclin E, a nuclear protein essential for the G1-to-S phase transition. *Mol. Cell. Biol.*, **15**(5), 2612–2624.

Peart, M. J., Poyurovsky, M. V., Kass, E. M., Urist, M., Verschuren, E. W., Summers, M. K., Jackson, P. K., and Prives, C. (2010). APC/C(Cdc20) targets E2F1 for degradation in prometaphase. *Cell cycle*, **9**(19), 3956–3964.

Rape, M. and Kirschner, M. W. (2004). Autonomous regulation of the anaphase-promoting complex couples mitosis to S-phase entry. *Nature*, **432**(7017), 588–595.

Rape, M., Reddy, S. K., and Kirschner, M. W. (2006). The Processivity of Multiubiquitination by the APC Determines the Order of Substrate Degradation. *Cell*, **124**(1), 89–103.

Remy, E., Rebouissou, S., Chaouiya, C., Zinovyev, A., Radvanyi, F., and Calzone, L. (2015). A Modeling Approach to Explain Mutually Exclusive and Co-Occurring Genetic Alterations in Bladder Tumorigenesis. *Cancer Res.*, **75**(19), 4042–4052.

Rivard, N., L'Allemain, G., Bartek, J., and Pouyssegur, J. (1996). Abrogation of p27Kip1 by cDNA antisense suppresses quiescence (G0 state) in fibroblasts. *J. Biol. Chem.*, **271**(31), 18337–18341.

Stoll, G., Viara, E., Barillot, E., and Calzone, L. (2012). Continuous time Boolean modeling for biological signaling: application of gillespie algorithm. *BMC Systems Biology*, **6**, 116.

Thomas, R. (1973). Boolean formalization of genetic control circuits. *J. Theor. Biol.*, **42**(3), 563–585.

Townsley, F. M., Aristarkhov, A., Beck, S., Hershko, A., and Ruderman, J. V. (1997). Dominant-negative cyclin-selective ubiquitin carrier protein E2-C/UbcH10 blocks cells in metaphase. *Proc. Natl. Acad. Sci. U.S.A.*, **94**(6), 2362–2367.

Tyson, J. J. and Novák, B. (2015). Models in biology: lessons from modeling regulation of the eukaryotic cell cycle. *BMC Biology*, **13**, 46.

Weinberg, R. A. (1995). The retinoblastoma protein and cell cycle control. *Cell*, **81**(3), 323–330.

Weis, M. C., Avva, J., Jacobberger, J. W., and Sreenath, S. N. (2014). A data-driven, mathematical model of mammalian cell cycle regulation. *PLoS ONE*, **9**(5), 1–13.

Wong, J. V., Dong, P., Nevins, J. R., Mathey-Prevot, B., and You, L. (2014). Control of E2F dynamics in cell cycle entry. *Cell Cycle*, **10**(18), 3086–3094.